# Synthesis, Characterization, and Second-Harmonic Generation Studies of Surfactant Rhenium(I) Diimine Complexes in Langmuir−Blodgett Films. X-ray Crystal Structure of *fac*-ClRe(CO)₃L (L = 9-Heptylamino-4,5-diazafluorene)

Vivian Wing-Wah Yam,* Ke-Zhi Wang, Chun-Ru Wang, Yu Yang, and
Kung-Kai Cheung

*Department of Chemistry, The University of Hong Kong, Pokfulam Road, Hong Kong*

A series of surfactant complexes of general formula, *fac*-ClRe(CO)₃L (L = 9-octadecylamino-4,5-diazafluorene, 9-(4′-hexadecylanilino)-4,5-diazafluorene, *N*-(4′-hexadecylphenyl)pyridine-2-carbaldimine, and 9-heptylamino-4,5-diazafluorene), were synthesized and characterized by elemental analyses and ¹H NMR, UV−vis, IR, and luminescence spectroscopy. The complex *fac*-ClRe(CO)₃L (L = 9-heptylamino-4,5-diazafluorene) was structurally characterized. The formation and optical properties of their Langmuir−Blodgett (LB) films were studied by surface pressure−area ($\pi$−A) isotherms and UV−vis and luminescence spectroscopy, and the second-harmonic generation (SHG) behavior was also investigated.

## Introduction

Rhenium(I) complexes of general formula *fac*-ClRe-(CO)₃L (L = α,α′-diimine) have been receiving growing interest in recent years, largely due to their potential uses as sensitizers and catalysts for solar energy conversion, electron-transfer reactions, and reduction of carbon dioxide in homogeneous solution and at electrode surfaces.[1−4] These complexes have been found to show attractive excited-state redox properties and intense luminescence in the visible region of the spectrum, are stable to photodecomposition,[5] and are well-suited for the applications addressed above.

The Langmuir−Blodgett technique is one of the powerful tools of making highly homogeneous, ordered ultrathin films for the development of future molecular devices.[6] The LB films based on metal complexes have been found to show interesting optical, electrical, and magnetic properties but so far have not been as well-explored as those of their organic counterparts.[7,8] As a d⁶ luminescent transition-metal system, Ru(II) surfactant complexes for LB films have been well investigated,[8] aimed at modification of properties such as those of film formation, luminescence and UV−vis spectroscopy, modified electrodes, photochemical cleavage of water into H₂ and O₂, and second-order nonlinear optical behavior.[8,9] However, surfactant Re(I) complexes for LB films have not been reported so far. To extend the types of compounds available for LB film studies and to increase their potential applications, a research program studying LB films of Re(I) complexes has been launched by our group.[10]

On the other hand, second-order nonlinear optical LB films have become one of the active fields of research

(1) (a) Geoffroy, G. L.; Wrighton, M. S. *Organometallic Photochemistry*; Academic Press: New York, 1979. (b) Zipp, A. P. *Coord. Chem. Rev.* **1988**, *84*, 47. (c) Meyer, T. J. *Pure Appl. Chem.* **1986**, *58*, 1193. (d) Caspar, J. V.; Sullivan, B. P.; Meyer, T. J. *Inorg. Chem.* **1984**, *23*, 2098. (e) Meyer, T. J. *Acc. Chem. Res.* **1989**, *22*, 163.

(2) (a) Balzani, V.; Moggi, L.; Scandola, F. *Supramolecular Photochemistry*; Reidel: Dordrecht, The Netherlands, 1987. (b) Balzani, V.; Scandola, F. *Supramolecular Photochemistry*; Ellis Horwood: Chichester, 1991. (c) Kavarnos, G. J. *Fundamentals of Photoinduced Electron Transfer*; VCH Publishers: New York, 1993.

(3) (a) Hawecker, J.; Lehn, J.-M.; Ziessel, R. *J. Chem. Soc., Chem. Commun.* **1983**, 536. (b) Sullivan, B. P.; Meyer, T. J. *J. Chem. Soc., Chem. Commun.* **1984**, 1244. (c) Sullivan, B. P.; Bolinger, C. M.; Conrad, D.; Vining, W. J.; Meyer, T. J. *J. Chem. Soc., Chem. Commun.* **1985**, 1414. (d) O'Toole, T. R.; Margerum, L. D.; Westmoreland, T. D.; Vining, W. J.; Murray, R. W.; Meyer, T. J. *J. Chem. Soc., Chem. Commun.* **1985**, 1416. (e) Caspar, J. V.; Sullivan, B. P.; Meyer, T. J. *Organometallics* **1986**, *5*, 1500.

(4) (a) Breikss, A. I.; Abruna, H. D. *J. Electroanal. Chem. Interfacial Electrochem.* **1986**, *201*, 347. (b) Cabrera, C. R.; Abruna, H. D. *J. Electroanal. Chem. Interfacial Electrochem.* **1986**, *209*, 101.

(5) (a) Lees, A. J. *Chem. Rev.* **1987**, 87, 711. (b) Sacksteder, L.; Zipp, A. P.; Brown, E. A.; Streich, J.; Demas, J. N.; DeGraff, B. A. *Inorg. Chem.* **1990**, *29*, 4335. (c) Wallace, L.; Rillema, D. P. *Inorg. Chem.* **1993**, *32*, 3836. (d) Schanze, K. S.; MacQueen, D. B.; Perkins, T. A.; Cabana, L. A. *Coord. Chem. Rev.* **1993**, *122*, 63.

(6) (a) Blodgett, B. *J. Am. Chem. Soc.* **1935**, *57*, 1007. (b) Roberts, G. G. *Langmuir−Blodgett Films*; Plenum Press: New York, 1990.

(7) (a) Huang, C. H.; Wang, K. Z.; Xu, G. X.; Xu, Y.; Liu, Y. Q.; Zhao, X. S.; Xie, X. M. *J. Phys. Chem.* **1995**, *99*, 14397. (b) Wang, K. Z.; Huang, C. H.; Xu, G. X.; Xu, Y.; Liu, Y. Q.; Zhao, X. S.; Xie, X. M. *Chem. Mater.* **1994**, *6*, 1986. (c) Wang, K. Z.; Huang, C. H.; Xu, G. X.; Zhao, X. S.; Xie, X. M. *Thin Solid Films* **1994**, *247*, 1. (d) Wang, K. Z.; Huang, C. H.; Xu, G. X.; Xu, L. G.; Li, T. K.; Zhao, X. S.; Xie, X. M. *Solid State Commun.* **1995**, *93*, 189. (e) Qian, D. J.; Nakahara, H. K.; Yang, K. *Chem. Lett.* **1995**, 175.

(8) (a) Delaive, P.; Lee, J. R.; Sprintschnik, H. W.; Abruna, H.; Meyer, T. J.; Whitten, D. G. *J. Am. Chem. Soc.* **1977**, *99*, 7094. (b) Gaines, G. L., Jr.; Behnken, P. E.; Valenty, S. J. *J. Am. Chem. Soc.* **1978**, *100*, 6549. (c) Valenty, S. J.; Behnken, D. E.; Gaines, G. L., Jr. *Inorg. Chem.* **1979**, *18*, 2160. (d) Daifuku, H.; Aoki, K.; Tokuda, K.; Matsuda, H. *J. Electroanal. Chem.* **1982**, *140*, 179. (e) Fujihira, M.; Nishiyama, K.; Yamada, H. *Thin Solid Films* **1985**, *132*, 77. (f) Daifuka, H.; Aoki, K.; Tokuda, K.; Matsuda, H. *J. Electroanal. Chem.* **1985**, *183*, 1. (g) Zhang, X.; Bard, A. J. *J. Phys. Chem.* **1988**, *92*, 5566. (h) Seefeld, K. P.; Mobius, D.; Kuhn, H. *Helv. Chim. Acta* **1977**, *60*, 2608.

(9) (a) Sakaguchi, H.; Nakamura, H.; Nagamura, T.; Ogawa, T.; Matsuo, T. *Chem. Lett.* **1989**, 1715. (b) Yamada, S.; Nakano, T.; Matsuo, T. *Thin Solid Films* **1994**, *245*, 196. (c) Sakaguchi, H.; Nakamura, H.; Nagamura, T.; Ogawa, T. Matsuo, T. *Jpn. J. Appl. Phys.* **1991**, *30*, 377.

due to their promising applications in photonic devices.[11] Most of the second-order nonlinear optical materials reported are of conventional donor−π-acceptor structures. Recently, strong second-harmonic generation from the LB films of surfactant Ru(II) complexes without the conventional donor−π-acceptor structures has been observed and attributed to metal-to-ligand charge-transfer (MLCT) excitation.[9] It was also found that several powder samples of Re(I) pyridine and bipyridine complexes had SHG efficiencies roughly comparable to urea (SHG at 532 nm). For example, [ReCl(CO)₃(2,2′-bipyridine)] had a powder efficiency of 1.7−2 times that of urea.[12]

Herein, we report the synthesis, characterization, and LB film studies of a series of new, robust, and easily accessible surfactant Re(I) complexes and the second-order nonlinear optical properties of these LB films.

## Experimental Section

**Materials.** Pyridine-2-carboxaldehyde (Aldrich) was distilled before use. Heptylamine (Aldrich) was distilled over KOH. Octadecylamine (98%, Aldrich), 4-hexadecylaniline (97%, Aldrich), and Re(CO)₅Cl (98%, Strem) were used as received. 4,5-Diazafluoren-9-one was prepared as reported previously.[13]

**Instrumentation and Equipment.** The UV−vis spectra were obtained on a Hewlett-Packard 8452A diode array spectrophotometer, IR spectra as Nujol mulls on a Bio-Rad FTS-7 spectrophotometer, and steady-state excitation and emission spectra on a Spex Fluorolog-2 111 spectrofluorometer with or without Corning filters. Low-temperature (77 K) spectra were recorded using an optical Dewar sample holder. Proton NMR spectra were recorded on a Bruker DPX-300 NMR spectrometer with chemical shifts reported relative to tetramethylsilane. Positive-ion fast-atom bombardment (FAB) and electron-impact (EI) mass spectra were recorded on a Finnigan MAT95 mass spectrometer. Elemental analyses were performed on a Carlo Erba 1106 elemental analyzer at the Institute of Chemistry, Chinese Academy of Sciences.

Emission lifetime measurements were made using a conventional laser system. The excitation source was the 355 nm output (third harmonic) of a Quanta-Ray Q-switched GCR-150-10 pulsed Nd:YAG laser. Luminescence decay signals were recorded on a Tektronix TDS 620A digital oscilloscope and analyzed using a program for exponential fits according to the equation $I(t) = I_0 \exp(-t/\tau)$, where $I(t)$ is the emission intensity at time $t$ after laser pulse and $I_0$ is the initial intensity at $t = 0$. All solutions for photophysical studies were prepared under vacuum in a 10-cm³ round-bottom flask equipped with a sidearm 1-cm fluorescence cuvette sealed from the atmosphere by a Kontes quick-release Teflon stopper. Solutions were rigorously degassed with no fewer than 4 freeze−pump−thaw cycles.

**Langmuir−Blodgett Films.** Ultrapure water (resistance > 18 MΩ cm) was obtained from an Elga UHQ PS apparatus and immediately used for LB film preparation. The complexes in chloroform (0.89 mg cm⁻³ for *fac*-ClRe(CO)₃**L1**, 1.38 mg cm⁻³ for *fac*-ClRe(CO)₃**L2**, and 1.0 mg cm⁻³ for *fac*-ClRe(CO)₃**L3**) were spread onto a pure water phase (pH 5.4, 18 °C) in a Nima model-622 computer-controlled trough. After a 15-min vaporization of the solvent, surface pressure−area (π−A) isotherms were recorded at a barrier compression speed of 150 cm² min⁻¹. The monolayers formed under a constant surface pressure (10 mN m⁻¹ for both *fac*-ClRe(CO)₃**L1** and *fac*-ClRe(CO)₃**L2** and 20 mN m⁻¹ for *fac*-ClRe(CO)₃**L3**) were transferred onto hydrophilically treated substrates of quartz after maintaining a constant pressure at the transfer pressure for 30 min for stabilization, at a dipping speed of 15 mm min⁻¹. The transfer ratios were close to unity. The substrates were made hydrophilic by consecutive sonication in detergent for 30 min and chloroform−ethanol for 15 min and soaking in both chromic acid and piranha solution[14] (30% H₂O₂−H₂SO₄, 3:7 v/v) for 8 h each before they were finally washed repeatedly with copious amounts of distilled and ultrapure water.

**Second-Harmonic Generation (SHG).** The setup for SHG was similar to that reported previously.[7a,b] The source was the fundamental 1064 nm light of a Quanta-Ray Q-switched GCR-150-10 pulsed Nd:YAG laser. The 532-nm light signals generated were recorded on a Tektronix TDS-620A digital oscilloscope. Prior to the SHG measurements, the monolayer films at the backsides of the substrates were wiped off carefully with lens tissues soaked in chloroform in order to prevent interference between signals arising from the monolayers at the front and backside of the substrate.

**Synthesis.** Synthetic schemes for the ligands and the rhenium(I) complexes are summarized in Scheme 1.

**Ligand Synthesis. 9-Octadecylamino-4,5-diazafluorene (L1). L1** was synthesized by modification of a literature method.[15] A mixture of octadecylamine (1.9 mmol), 4,5-diazafluoren-9-one (1.8 mmol), and 4-toluenesulfonic acid (0.013 g, 0.068 mmol) was dissolved in 20 mL of toluene. The mixture was refluxed in an oil bath for 24 h, during which a Dean−Stark apparatus was used to drive the reaction. Most of the solvent was then driven off under reduced pressure in a water bath. Petroleum ether (40−60 °C) was added with vigorous stirring until the solution became cloudy. On cooling in a refrigerator overnight, the precipitate formed was filtered off and characterized as mainly unreacted 4,5-diazafluoren-9-one. The filtrate was then evaporated to dryness, and the residue was recrystallized twice from petroleum ether (60−80 °C) to afford the desired product (0.28 g). Yield: 63%. Mp: 79.5 °C. ¹H NMR (300 MHz, CDCl₃, relative to Me₄Si): δ 8.75 (m, 2H), 8.18 (m, 2H), 7.34 (m, 2H), 4.18 (t, 2H, J = 7.1 Hz), 1.94 (m, 2H), 1.54 (m, 2H), 1.26 (m, 28H), 0.88 (t, 3H, J = 6.7 Hz). UV−vis (CHCl₃, λ/nm (ε × 10⁻³/dm³ mol⁻¹ cm⁻¹)): 306 (8.90), 316 (9.75). EI-MS *m/z*: 443 (M⁺). Anal. Calcd for C₂₉H₄₃N₃: C, 80.37; H, 9.93; N, 9.70. Found: C, 80.52; H, 10.1; N, 9.80.

**9-(4′-hexadecylanilino)-4,5-diazafluorene (L2). L2** was synthesized as described for **L1** except that 4-hexadecylaniline was used instead of octadecylamine. The product was purified by recrystallization from dichloromethane−petroleum ether twice (40−60 °C). Yield: 79%. Mp: 107 °C. ¹H NMR (300 MHz, CDCl₃, relative to Me₄Si): δ 8.80 (m, 1H), 8.64 (m, 1H), 8.25 (m, 1H), 7.40 (m, 1H), 7.24 (d, 2H, J = 8.4 Hz), 6.96 (m, 4H), 2.67 (t, 2H, J = 7.7 Hz), 1.26 (m, 28H), 0.88 (t, 3H, J = 6.4 Hz). UV−vis (CHCl₃, λ/nm (ε × 10⁻³/dm³ mol⁻¹ cm⁻¹)): 306 (8.02), 316 (8.01), 424 (1.50). EI-MS *m/z*: 481 (M⁺). Anal. Calcd for C₃₃H₄₃N₃: C, 82.33; H, 8.94; N, 8.73. Found: C, 82.19; H, 9.03; N, 8.52.

(10) (a) Yam, V. W. W.; Lau, V. C. Y.; Wang, K. Z.; Cheung, K. K.; Huang, C. H. *J. Mater. Chem.* **1998**, *8*, 89. (b) Lau, V. C. Y. Ph.D. Thesis, The University of Hong Kong, 1997.

(11) (a) *Materials for Nonlinear Optics, Chemical Perspectives*; Marder, S. R.; Sohn, J. E.; Stucky, G. D., Eds.; ACS Symp. Series; American Chemical Society: Washington, DC, 1991; p 455. (b) Prasad, P. N.; Williams, D. J. *Introduction to Nonlinear Optical Effects in Molecules and Polymers*; Wiley: New York, 1991. (c) Marks, T. J.; Ratner, M. A. *Angew. Chem., Int. Ed. Engl.* **1995**, *34*, 155. (d) Green, M. L. H.; Marder, S. R.; Thompson, M. E. *Nature* **1987**, *330*, 108. (e) Richardson, T.; Roberts, G. G.; Polywka, M. E. C.; Davies, S. G. *Thin Solid Films* **1989**, *179*, 405.

(12) (a) Calabrese, J. C.; Tam, W. *Chem. Phys. Lett.* **1987**, *133*, 244. (b) Anderson, A. G.; Calabrese, J. C.; Tam, W.; Williams, I. D. *Chem. Phys. Lett.* **1987**, *134*, 392.

(13) Henderson, L. J. Jr.; Fronczek, F. R.; Cherry, W. R. *J. Am. Chem. Soc.* **1984**, *106*, 5876.

(14) Ulman, A. *Ultrathin Organic Films*; Academic Press: Boston, 1991; p 108.

(15) Tai, Z. H.; Zhang, G. C.; Qian, X. P.; Xiao, S. J.; Lu, Z. H.; Wei, Y. *Langmuir* **1993**, *9*, 1601.

## Scheme 1.   Synthetic Routes of Ligands and Corresponding Surfactant Re(I) Complexes
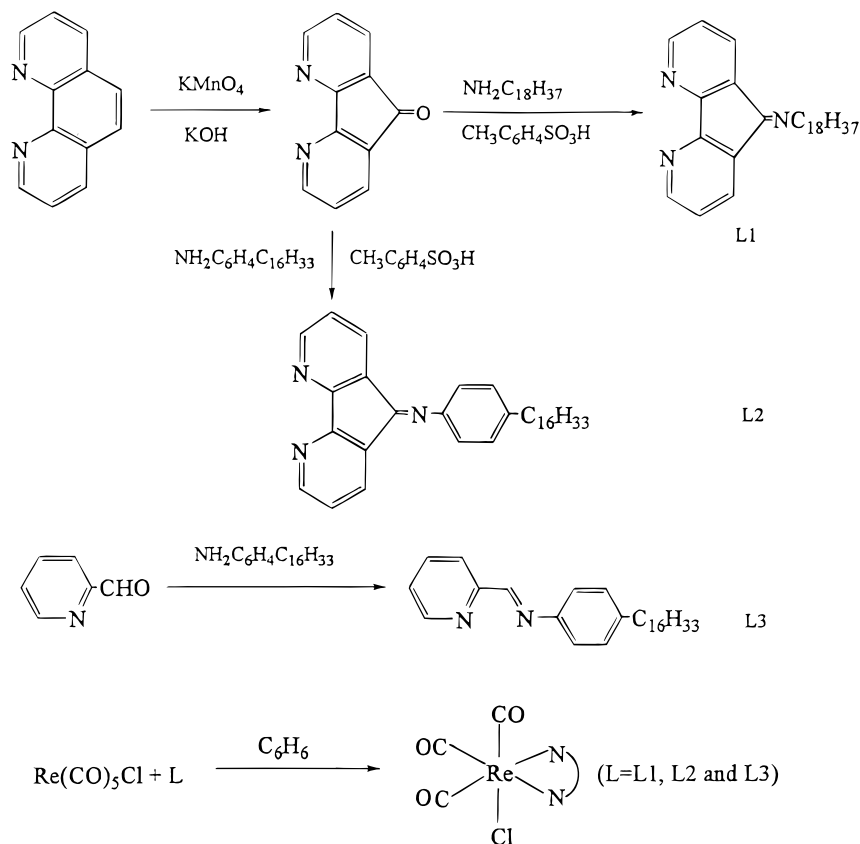
***N*-(4′-Hexadecylphenyl)pyridine-2-carbaldimine (L3).** **L3** was synthesized by modification of a literature procedure[16] by the condensation of pyridine-2-carboxaldehyde with hexadecylaniline overnight in ethanol in the presence of a catalytic amount of glacial acetic acid. The precipitate formed on cooling was recrystallized from ethanol. Removal of any colored impurities could be accomplished by column chromatography on silica gel using diethyl ether as the eluent. Yield: 87%. Mp: 43 °C. $^1$H NMR (300 MHz, CDCl$_3$, relative to Me$_4$Si): $\delta$ 8.70 (d, 1H, $J$ = 4.9 Hz), 8.64 (s, 1H), 8.20 (d, 1H, $J$ = 7.9 Hz), 7.83 (m, 1H), 7.38 (m, 1H), 7.26 (m, 4H), 2.63 (t, 2H, $J$ = 7.7 Hz), 1.63 (m, 2H), 1.26 (m, 26H), 0.88 (t, 3H, $J$ = 6.7 Hz). UV−vis (CHCl$_3$, $\lambda$/nm ($\epsilon \times 10^{-3}$/dm$^3$ mol$^{-1}$ cm$^{-1}$)): 286 (9.17), 332 (8.47). EI-MS $m/z$: 408 ({M + 2}$^+$). Anal. Calcd for C$_{28}$H$_{42}$N$_2$: C, 82.72; H, 10.35; N, 6.90. Found: C, 82.85; H, 10.74; N, 6.68.

**9-Heptylamino-4,5-diazafluorene (L4).** **L4** was synthesized as described for **L1** except heptylamine was used instead of octadecylamine. Yield: 65%. Mp: 84 °C. $^1$H NMR (300 MHz, CDCl$_3$, relative to Me$_4$Si): $\delta$ 8.74 (m, 2H), 8.17 (m, 2H), 7.33 (m, 2H), 4.17 (t, 2H, $J$ = 7.1 Hz), 1.94 (m, 2H), 1.59 (m, 2H), 1.35 (m, 6H), 0.90 (t, 3H, $J$ = 6.5 Hz). $^1$H NMR (300 MHz, CD$_3$CN, relative to Me$_4$Si): $\delta$ 8.70 (s, 2H), 8.31 (d, 1H, $J$ = 7.3 Hz), 8.06 (d, 1H, $J$ = 7.5 Hz), 7.40 (m, 2H), 4.16 (t, 2H, $J$ = 6.5 Hz), 1.88 (m, 2H), 1.53 (m, 2H), 1.34 (m, 6H), 0.90 (t, 3H, $J$ = 6.8 Hz). EI-MS $m/z$: 280 ({M + 1}$^+$).

**Synthesis of Rhenium(I) Diimine Complexes.** ***fac*-ClRe(CO)$_3$L (L = L1, L2, L3, and L4).** These complexes were synthesized by modification of a literature procedure.[17] A mixture of Re(CO)$_5$Cl (54.3 mg, 0.15 mmol) and L (0.15 mmol) in 8 mL of benzene was heated to reflux under N$_2$ for

2 h. After removal of the solvent, the residue was triply recrystallized from CH$_2$Cl$_2$−hexane. Yield: 80%. Slow diffusion of diethyl ether vapor into an acetonitrile solution of *fac*-ClRe(CO)$_3$**L4** afforded pale yellow platelike crystals suitable for X-ray crystallographic studies.

***fac*-ClRe(CO)$_3$L1.** Mp: 129 °C. $^1$H NMR (300 MHz, CDCl$_3$, relative to Me$_4$Si): $\delta$ 8.80 (t, 2H, $J$ = 5.5 Hz), 8.31 (t, 2H, $J$ = 8.4 Hz), 7.60 (m, 2H), 4.24 (t, 2H, $J$ = 7.0 Hz), 1.95 (m, 2H), 1.26 (m, 30H), 0.88 (t, 3H, $J$ = 6.4 Hz). UV−vis (CH$_2$Cl$_2$, $\lambda$/nm ($\epsilon \times 10^{-4}$/dm$^3$ mol$^{-1}$ cm$^{-1}$)): 322 (2.86), 382 (0.69). UV−vis (LB film, $\lambda$/nm): 324. IR (Nujol, $\nu$/cm$^{-1}$): 2033 (s) $\nu$(CO), 1928 (s) $\nu$(CO), 1888 (vs) $\nu$(CO). Positive FAB-MS $m/z$: 739 (M$^+$); 704 ({M − Cl}$^+$). Anal. Calcd for C$_{32}$H$_{43}$N$_3$O$_3$ClRe·0.5H$_2$O: C, 51.34; H, 5.88; N, 5.61. Found: C, 51.29; H, 5.64; N, 5.57.

***fac*-ClRe(CO)$_3$L2.** Mp: 138 °C. $^1$H NMR (300 MHz, CDCl$_3$, relative to Me$_4$Si): $\delta$ 8.84 (d, 1H, $J$ = 7.3 Hz), 8.71 (d, 1H, $J$ = 5.2 Hz), 8.41 (d, 1H, $J$ = 7.7 Hz), 7.66 (t, 1H, $J$ = 7.3 Hz), 7.30 (d, 2H, $J$ = 8.1 Hz), 7.27 (m, 1H), 7.20 (d, 1H, $J$ = 7.8 Hz), 6.98 (d, 2H, $J$ = 8.0 Hz), 2.70 (t, 2H, $J$ = 7.6 Hz), 1.69 (m, 2H), 1.27 (m, 26H), 0.88 (t, 3H, $J$ = 6.5 Hz). UV−vis (CH$_2$Cl$_2$, $\lambda$/nm ($\epsilon \times 10^{-4}$/dm$^3$ mol$^{-1}$ cm$^{-1}$)): 322 (1.49), 414 (0.56). UV−vis (LB film, $\lambda$/nm): 328. IR (Nujol, $\nu$/cm$^{-1}$): 2038 (s) $\nu$(CO) 1926 (vs) $\nu$(CO), 1867 (s) $\nu$(CO). Positive FAB-MS $m/z$: 787 (M$^+$); 752 ({M − Cl}$^+$). Anal. Calcd for C$_{36}$H$_{43}$ClN$_3$O$_3$-Re·0.5H$_2$O: C, 54.27; H, 5.53; N, 5.28. Found: C, 54.42; H, 5.35; N, 5.26.

***fac*-ClRe(CO)$_3$L3.** Mp: 111 °C. $^1$H NMR (300 MHz, CDCl$_3$, relative to Me$_4$Si): $\delta$ 9.10 (d, 1H, $J$ = 5.4 Hz), 8.77 (s, 1H), 8.10 (m, 1H), 8.00 (d, 1H, $J$ = 7.5 Hz), 7.63 (m, 1H), 7.44 (d, 2H, $J$ = 8.4 Hz), 7.30 (d, 2H, $J$ = 8.3 Hz), 2.68 (t, 2H, $J$ = 7.8 Hz), 1.64 (m, 2H), 1.26 (m, 26H), 0.88 (t, 3H, $J$ = 6.6 Hz). UV−vis (CH$_2$Cl$_2$, $\lambda$/nm ($\epsilon \times 10^{-4}$/dm$^3$ mol$^{-1}$ cm$^{-1}$): 348 (1.63), 426 (0.69). UV−vis (LB film, $\lambda$/nm): 352, 434. IR (Nujol, $\nu$/cm$^{-1}$): 2023 (s) $\nu$(CO), 1928 (vs) $\nu$(CO), 1895 (vs) $\nu$(CO). Positive FAB-MS $m/z$: 712 (M$^+$), 677 ({M − Cl}$^+$). Anal. Calcd for

(16) Johnson, D. W.; Mayer, H. K.; Minard, J. P.; Banatida, J.; Miller, C. *Inorg. Chim. Acta* **1988**, *144*, 167.
(17) (a) Wrighton, M. S.; Morse, D. L. *J. Am. Chem. Soc.* **1974**, *96*, 998. (b) Dominey, R. N.; Hauser, B.; Hubbard, J.; Dunham, J. *Inorg. Chem.* **1991**, *30*, 4754. (c) Caspar, J. V.; Meyer, T. J. *J. Phys. Chem.* **1983**, *87*, 952.

**Table 1. Selected Bond Distances (Å) and Bond Angles (deg) for Complex *fac*-ClRe(CO)₃L4**

| Distances | | | |
|---|---|---|---|
| Re–Cl(1) | 2.471(2) | Re–N(1) | 2.230(5) |
| Re–N(2) | 2.233(5) | Re–C(1) | 1.911(7) |
| Re–C(2) | 1.900(7) | Re–C(3) | 1.921(7) |

| Angles | | | |
|---|---|---|---|
| Cl(1)–Re–N(1) | 82.5(1) | Cl(1)–Re–N(2) | 83.4(1) |
| Cl(1)–Re–C(1) | 89.7(2) | Cl(1)–Re–C(2) | 94.9(2) |
| Cl(1)–Re–C(3) | 176.0(2) | N(1)–Re–N(2) | 78.3(2) |
| N(1)–Re–C(1) | 171.2(2) | N(1)–Re–C(2) | 93.9(2) |
| N(1)–Re–C(3) | 96.6(2) | N(2)–Re–C(1) | 96.8(2) |
| N(2)–Re–C(2) | 172.1(2) | N(2)–Re–C(3) | 92.6(2) |
| C(1)–Re–C(2) | 90.8(3) | C(1)–Re–C(3) | 90.8(3) |
| C(2)–Re–C(3) | 89.1(3) | | |

$C_{31}H_{42}N_2ClO_3Re$: C, 52.27; H, 5.90; N, 3.93. Found: C, 52.25; H, 5.76; N, 3.58.

***fac*-ClRe(CO)₃L4.** Mp: 171 °C. $^1$H NMR (300 MHz, CDCl₃, relative to Me₄Si): δ 8.80 (t, 2H, $J$ = 5.5 Hz), 8.31 (t, 2H, $J$ = 8.8 Hz), 7.60 (m, 2H), 4.24 (t, 2H, $J$ = 7.0 Hz), 1.95 (m, 2H), 1.26 (m, 8H), 0.91 (t, 3H, $J$ = 6.5 Hz). UV–vis (CH₂Cl₂, $\lambda$/nm ($\epsilon \times 10^{-4}$/dm³ mol⁻¹ cm⁻¹)): 322 (1.24), 382 (0.28). IR (Nujol, $\nu$/cm⁻¹): 2025 (vs) $\nu$(CO), 1921 (vs) $\nu$(CO), 1890 (vs) $\nu$(CO). Positive FAB-MS $m/z$: 585 (M⁺), 550 ({M – Cl}⁺). Anal. Calcd for $C_{21}H_{21}ClN_3O_3Re$: C, 43.08; H, 3.59; N, 7.18. Found: C, 43.30; H, 3.49; N, 7.16.

**Crystallographic Work.** Crystal data: [ReClO₃N₃C₂₁H₂₁], $M_r$ = 585.08, triclinic, space group $P\bar{1}$ (No. 2), $a$ = 9.767(1) Å, $b$ = 10.934(3) Å, $c$ = 12.153(4) Å, $\alpha$ = 108.87(2)°, $\beta$ = 95.26-(2)°, $\gamma$ = 115.11(1)°, $V$ = 1071.6(6) Å³, $Z$ = 2, $D_C$ = 1.813 g cm⁻³, (Mo K$\alpha$) = 58.23 cm⁻¹, $F(000)$ = 568, $T$ = 298 K. A pale yellow crystal of dimensions 0.45 × 0.20 × 0.08 mm was used for data collection at 25 °C on an Enraf-Nonius CAD4 diffractometer with graphite-monochromated Mo K$\alpha$ radiation ($\lambda$ = 0.710 73 Å) using $\omega$–2$\theta$ scans with a $\omega$-scan angle (0.65 + 0.35 tan $\theta$)° at a scan speed of 1.37–5.49 deg min⁻¹. Intensity data (in the range of 2$\theta_{max}$ = 48°; $h$, 0 to 11; $k$, –12 to 12; $l$, –13 to 13; and three standard reflections measured after every 300 reflections showed decay of 3.98%) were corrected for decay, Lorentz and polarization effects, and empirical absorption corrections based on the $\Psi$-scan of four strong reflections (minimum and maximum transmission factors 0.354 and 1.000). Upon averaging the 3586 reflections, 3361 of which were uniquely measured ($R_{int}$ = 0.029), 3169 reflections with $I > 3\sigma(I)$ were considered observed and used in the structural analysis. The centric space group was based on a statistical analysis of intensity distribution, and the successful solution and refinement of the structure was solved by direct methods (SIR92[18a]), expanded by Fourier methods and refined by full-matrix least-squares using the software package TeXsan[18b] on a Silicon Graphics Indy computer. A crystallographic asymmetric unit comprised of one molecule and all 29 non-H atoms of the molecule were refined anisotropically. Twenty-one H atoms of the complex at calculated positions with thermal parameters equal to 1.3 times that of the attached C atoms were not refined. Convergence for 262 variable parameters by least-squares refinement on $F$ with $w = 4F_o^2/\sigma^2(F_o^2)$, where $\sigma^2(F_o^2) = [\sigma^2(I) + (0.035F_o^2)^2]$ for 3169 reflections with $I > 3\sigma$-($I$), was reached at $R$ = 0.037 and $R_w$ = 0.046 with a goodness-of-fit of 2.25. $(\Delta/\sigma)_{max}$ = 0.02. The final difference Fourier map was featureless, with maximum positive and negative peaks of 3.42 and –1.00 e Å⁻³, respectively. The positive peak was in the vicinity of the Re atom. The atomic coordinates, thermal parameters, and bond lengths are given in the Supporting Information. Selected bond distances and angles for complex *fac*-ClRe(CO)₃L4 are given in Table 1.
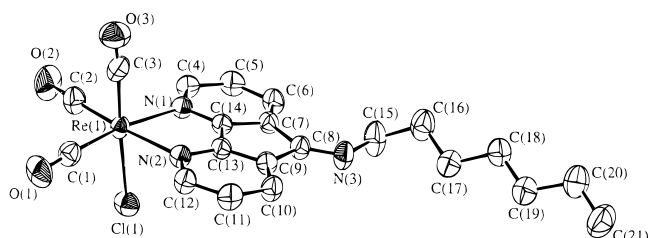


**Figure 1.** Perspective drawing of the complex *fac*-ClRe-(CO)₃**L4** with atomic numbering scheme. Hydrogen atoms have been omitted for clarity. The thermal ellipsoids are shown at the 40% probability levels.

## Results and Discussion

**Syntheses.** Ligand **L1** was first synthesized by Tai et al.[15] in which BF₃ was used as the catalyst. We modified the procedure with the use of the more easily handled solid 4-toluenesulfonic acid as the catalyst instead of BF₃ to give **L1** and **L2** in good and reproducible yields. The Re(I) complexes were subsequently synthesized by a slight modification of a literature method,[17] by the reaction of stoichiometric amounts of Re(CO)₅Cl and L in refluxing benzene under an inert atmosphere of nitrogen to afford *fac*-ClRe(CO)₃L. All of the newly synthesized complexes gave satisfactory elemental analysis and were characterized by IR, UV–vis, positive FAB-MS, and $^1$H NMR spectroscopy. The IR spectra of the complexes show three intense absorption bands in the region 1860–2040 cm⁻¹, typical of the facial arrangement of the three carbonyl groups.[19] The structure of *fac*-ClRe(CO)₃**L4** was also determined by X-ray crystallography.

**Crystal Structure.** A perspective drawing of the structure of the complex *fac*-ClRe(CO)₃**L4** with atomic numbering is shown in Figure 1. The coordination geometry at the Re atom is distorted octahedral with the three carbonyl ligands arranged in a facial fashion. The N(1)–Re–N(2) bond angle of 78.3° (less than 90°) is a result of the steric requirement of the bidentate diimine ligand. All other bond distances and bond angles are not remarkable and are comparable to those found for the related rhenium(I) polypyridyl complexes.[20,21]

**Surface Pressure–Area ($\pi$–A) Isotherms.** $\pi$–A isotherms for the Re(I) complexes are shown in Figure 2. The complexes showed stable monolayer film-forming properties and had two well-defined phase transitions. Compression–expanding cycles showed that the first phase transition at the lower surface pressure is associated with monolayer film formation from gaseous phase and the other one at high surface pressure is

(18) (a) *SIR92*: Altomare, A.; Cascarano, M.; Giacovazzo, C.; Guagliardi, A.; Burla, M. C.; Polidori, G.; Camalli, M. *J. Appl. Crystallogr.* **1994**, *27*, 435. (b) *TeXsan*: *Crystal Structure Analysis Package*; Molecular Structure Corp., 1985 and 1992.

(19) Giordano, P. J.; Wrighton, M. S. *J. Am. Chem. Soc.* **1979**, *101*, 2888.

(20) (a) Lees, A. J. *Comm. Inorg. Chem.* **1995**, *17*, 319. (b) Moya, S. A.; Guerrero, J.; Pastene, R.; Schmidt, R.; Sariego, R.; Sartori, R.; Sanz-Aparicio, J.; Fonseca, I.; Maertiez-Ripoll, M. *Inorg. Chem.* **1994**, *33*, 2341. (c) Abel, E. W.; Dimitrov, V. S.; Long, N. J.; Orrel, K. G.; Osborne, A. G.; Pain, H. M.; Hursthouse, M. B.; Mazid, M. A. *J. Chem. Soc., Dalton Trans.* **1993**, 597. (d) Civitello, E. R.; Dragovich, P. S.; Karpishin, T. B.; Novick, S. G.; Bierach, G.; O'Connell, J. F.; Westmoreland, T. D. *Inorg. Chem.* **1993**, *32*, 237. (e) Porter, L. H.; Reid, A. H.; Fackler, J. P., Jr. *Acta Crystallogr.* **1992**, *48*, 908.

(21) (a) Yam, V. W.-W.; Lau, V. C.-Y.; Cheung, K. K. *Organometallics* **1995**, *14*, 2749. (b) Yam, V. W.-W.; Lau, V. C.-Y.; Cheung, K. K. *J. Chem. Soc., Chem. Commun.* **1995**, 259. (c) Yam, V. W.-W.; Lo, K. K. W.; Cheung, K. K.; Kong, R. Y. C. *J. Chem. Soc., Chem. Commun.* **1995**, 1191. (d) Yam, V. W.-W.; Lo, K. K. W.; Cheung, K. K.; Kong, R. Y. C. *J. Chem. Soc., Dalton Trans.* **1997**, 2067.
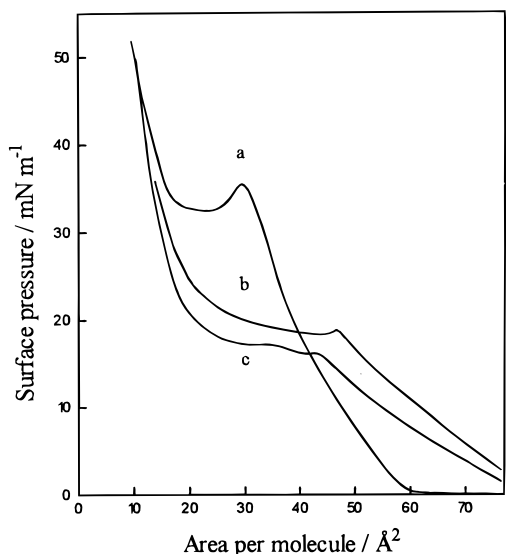
**Figure 2.** Surface pressure−area ($\pi$−A) isotherms: (a) ReCl(CO)$_3$**L3**; (b) ReCl(CO)$_3$**L1**; (c) ReCl(CO)$_3$**L2**.



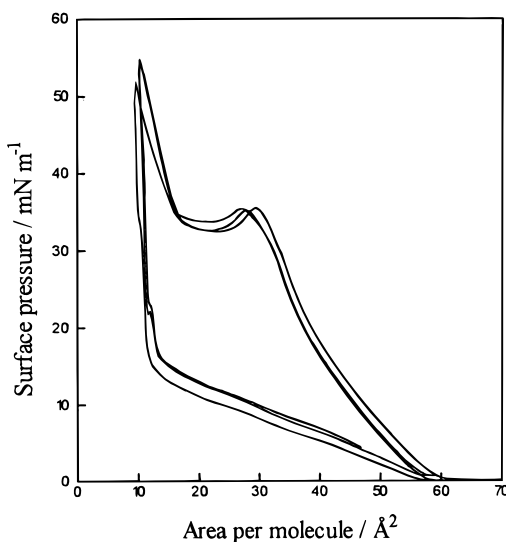**Figure 3.** Compression−expanding isotherms for ReCl-(CO)$_3$**L3**.

related to the formation of aggregates or multilayer films from the monolayer film. This can be seen from the compression−expanding cycle of *fac*-ClRe(CO)$_3$**L3** as shown in Figure 3. A large hysteresis appeared when the reverse pressure is larger than the critical phase transition point. However, the $\pi$−A isotherms could be reversibly compressed and expanded when the reverse pressure was lower than the critical phase transition point. The molecular area for *fac*-ClRe(CO)$_3$**L3** obtained by extrapolation from the linear region of the first phase transition at the lower surface pressure is 0.48 nm$^2$, which agrees well with the calculated value of 0.5 nm$^2$, considering that both the N-containing ligand plane and the long alkyl chain are oriented vertically with respect to the water surface, with the molecules closely packed in the films. On the contrary, the molecular area of the other two complexes *fac*-ClRe(CO)$_3$**L1** and *fac*-ClRe-(CO)$_3$**L2** are much larger than the calculated value, indicating that the alkyl chains were highly tilted in their films. In addition, the region associated with monolayer film formation in the $\pi$−A curves for *fac*-ClRe(CO)$_3$**L1** and *fac*-ClRe(CO)$_3$**L2** is not as steep as
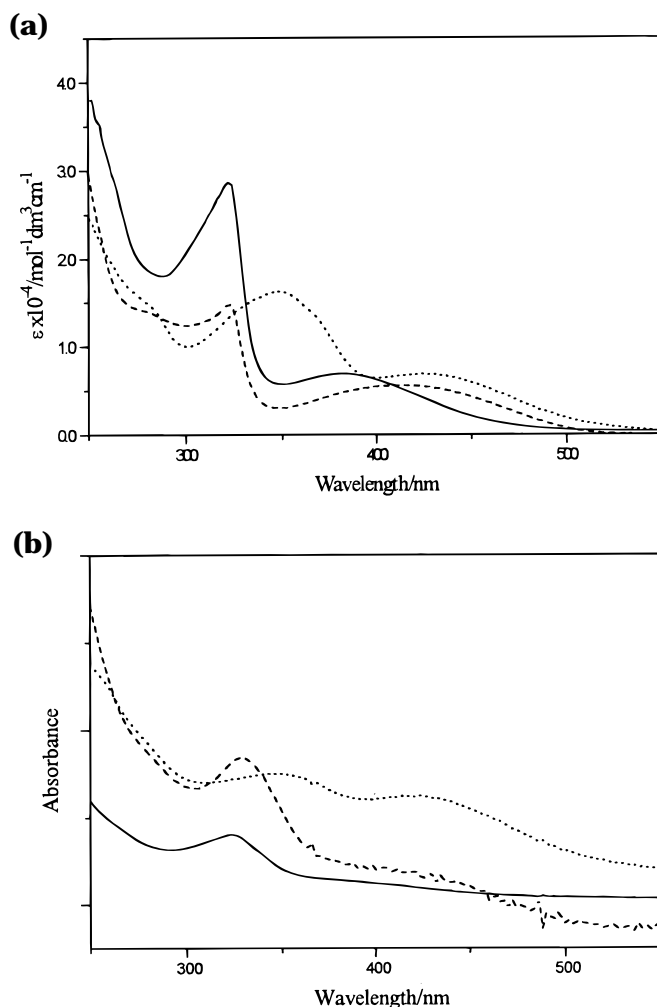




**Figure 4.** UV−vis spectra of ReCl(CO)$_3$**L1** (—), ReCl-(CO)$_3$**L2** (- - -), and ReCl(CO)$_3$**L3**($\cdots$): (a) in CH$_2$Cl$_2$, (b) in LB film.

that observed for *fac*-ClRe(CO)$_3$**L3**, indicative of their poorer film-formation property compared to *fac*-ClRe-(CO)$_3$**L3**.

**UV−Vis Absorption Spectra.** The UV−vis absorption spectra of the rhenium(I) complexes showed intense absorption bands at ca. 300−350 nm, attributable to ligand-centered transitions, and a broad band at ca. 380−430 nm, which is attributed to a metal-to-ligand charge transfer (MLCT, d$\pi$ (Re) → $\pi$*(L)) transition.[1−3,5,17,20,21] The only exception is ClRe(CO)$_3$**L2**, where the low-energy absorption at ca. 414 nm is attributed to an admixture of intraligand (IL, $\pi$ → $\pi$*-(**L2**)) and metal-to-ligand charge transfer (MLCT, d$\pi$ (Re) → $\pi$*(**L2**)) transitions, in view of the presence of the low-energy IL band at ca. 420 nm in the free ligand **L2**. Both ClRe(CO)$_3$**L2** and ClRe(CO)$_3$**L3** absorbed at lower energies than ClRe(CO)$_3$**L1**, in line with the lower-lying $\pi$* orbital energy of the more conjugated **L2** and **L3** ligands. Figure 4 shows the UV−vis spectra of the complexes in LB film and in chloroform solution. The absorption patterns are similar with those in LB film having less features than those in chloroform solution, indicative of the presence of aggregates in the LB films.[22] The UV−vis spectra of *fac*-ClRe(CO)$_3$**L3** in LB films are found to show a linear dependence of

(22) Chen, H.; Law, K.-Y.; Whitten, D. G. *J. Phys. Chem.* **1996**, *100*, 5949.

**Table 2.  Emission Data for the Rhenium(I) Complexes *fac*-ClRe(CO)₃L**

| L | CH₂Cl₂ (298 K), $\lambda_{em}$/nm ($\tau_0/\mu s$) | CHCl₃ glass (77 K), $\lambda_{em}$/nm | LB film, $\lambda_{em}$/nm |
|---|---|---|---|
| **L1** | 595 (0.10) | 555 | 575 |
| **L2** | 590 (0.30) | 535 | *a* |
| **L3** | 720 (<0.02) | 645 | 660 |

*a* Not measured.
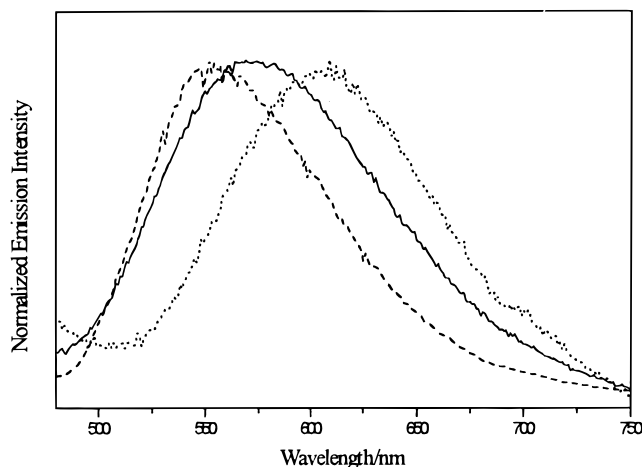


**Figure 5.**  Normalized emission spectra (—, LB film; - - -, complex at glassy state (77 K); ···, complex in CH₂Cl₂) of ReCl(CO)₃**L1**.

absorbance on the number of layers deposited, indicative of its good deposition behavior.  On the contrary, the complexes *fac*-ClRe(CO)₃**L1** and *fac*-ClRe(CO)₃**L2** were found to show poor deposition behavior which became irreproducible after the deposition of five layers.

**Luminescence Spectra.**  Emission data for the complexes in various media are summarized in Table 2, and the emission spectra of ClRe(CO)₃**L1** are shown in Figure 5.  The emission spectra exhibited a broad unstructured emission band, attributed to a triplet MLCT-based emission, typical of Re(I) diimine complexes.[1-3,5,17,20,21,23]  The emission energies of the complexes in 77 K glass and in LB films were found to be blue-shifted with respect to that in fluid solutions, attributed to the phenomenon of luminescence rigidochromism.[5a,19,24]

**Second-Harmonic Generation (SHG).**  For conventional nonlinear optical (NLO) organic compounds, the NLO property originated from intramolecular charge transfer and the second-order molecular hyperpolarizability ($\beta$) is dominated by the component along the intramolecular donor−π-acceptor axis.  In 1989, SHG from LB films of Ru(II) complexes was first observed[9] and subsequently verified to result from a d$\pi$(Ru) → $\pi$*(bpy) metal-to-ligand charge transfer excited state with the transition dipole moment mainly oriented along the 2,2′-bipyridine moiety attached to the long alkyl chain.  In the SHG measurements, the monolayer film of *fac*-ClRe(CO)₃**L3** has been shown to exhibit very
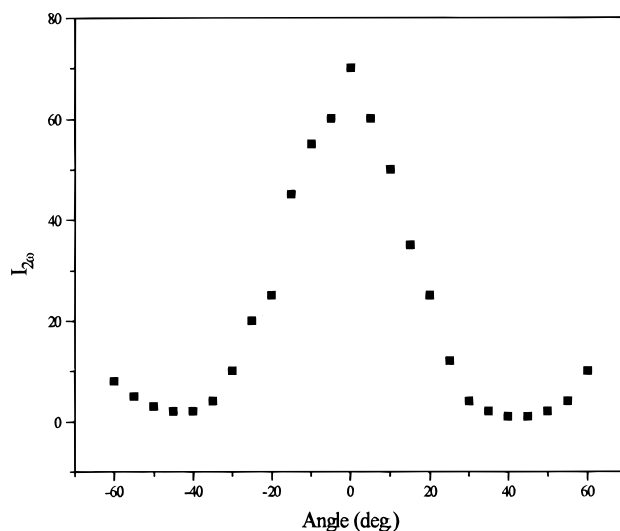


**Figure 6.**  Polarization dependence of the SHG (arbitrary units) from monolayer films of ReCl(CO)₃**L3**; the peak and troughs correspond to the signal from the *p*-polarized and *s*-polarized fundamental beams, respectively.  The abscissa corresponds to the angle of rotation of the half-wave plate.

strong second-harmonic (SH) signals.  A similar mechanism of second-harmonic generation to that of the Ru(II) complexes may operate in the amphiphilic Re complexes studied, and assuming that the MLCT transition moments have a common tilt angle, $\phi$, to the surface normal, with a random azimuthal distribution, and that second-order molecular hyperpolarizability ($\beta$) is dominated by the component along the MLCT axis, the following eqs 1−3 can be derived.[25]

$$I_{2\omega}(p \to p)/I_{2\omega}(s \to p) = (\chi^{(2)}(zzz)sin^3\,\theta + 3\chi^{(2)}(zxx)sin\,\theta\,cos^2\,\theta)^2 / (\chi^{(2)}(zxx)sin\,\theta)^2 \quad (1)$$

$$\chi^{(2)}(zzz) = \chi^{(2)}cos^3\,\phi = Nf_{2\omega}(f_\omega)^2\beta\,cos^3\,\phi \quad (2)$$

$$\chi^{(2)}(zxx) = 0.5\chi^{(2)}\,cos\,\phi\,sin^2\,\phi = 0.5Nf_{2\omega}(f_\omega)^2\beta\,cos\,\phi\,sin^2\,\phi \quad (3)$$

Substitution of eqs 2 and 3 into eq 1 gives eq 4 for the calculation of $\phi$:

$$tan\,\phi = [(I_{2\omega}(p \to p)/I_{2\omega}(s \to p))^{1/2} - {}^3/_2]^{-1/2} \quad (4)$$

where $I_{2\omega}(p \to p)$ is the *p*-polarized double-frequency signal intensity with p-polarized incidental fundamental light; $I_{2\omega}(s \to p)$ is *s*-polarized double-frequency signal intensity with *p*-polarized incidental fundamental light; *s* and *p* stand for perpendicular and parallel to the plane of incidence.

In the SHG experiment, the monolayer film of *fac*-ClRe(CO)₃**L3** showed strong SH signals and evident polarization dependence (Figure 6).  By a comparison of the signal to that obtained from a Y-cut quartz crystal reference ($d_{11} = 1.2 \times 10^{-9}$ esu),[26] $\chi^{(2)}$ and $\beta$ can be

(23) (a) Tapolsky, G.; Duesing, R.; Meyer, T. J. *Inorg. Chem.* **1990**, *29*, 2285. (b) Shaw, J. P.; Schmehl, R. H. *J. Am. Chem. Soc.* **1991**, *113*, 389. (c) Lin, R.; Fu, Y.; Brock, C. P.; Guarr, T. F. *Inorg. Chem.* **1992**, *31*, 4346. (d) Yoon, K. I.; Berg-Brennan, C. A.; Lu, H.; Hupp, J. T. *Inorg. Chem.* **1992**, *31*, 3192.
(24) (a) Kotch, T. G.; Lees, A. J. *Inorg. Chem.* **1993**, *32*, 2570. (b) Moya, S. A.; Schmidt, R.; Pastene, R.; Sartori, R.; Muller, U.; Frenzen, G. *Organometallics* **1996**, *15*, 3465.

(25) Ashwell, G. J.; Hargreaves, R. C.; Baldwin, C. E.; Bahra, C. S.; Brown, C. R. *Nature* **1992**, *357*, 393.
(26) (a) Jerphagnon, J.; Kurtz, S. K. *J. Appl. Phys.* **1970**, *41*, 1667. (b) Levine, B. F.; Bethea, C. G.; Thurmond, C. D.; Lynch, R. T.; Bernstein, J. L. *J. Appl. Phys.* **1979**, *50*, 2533. (c) Bloembergen, N.; Pershan, P. S. *Phys. Rev.* **1962**, *128*, 602.

**Table 3.   $\chi^{(2)}$, $\beta$, and Tilt Angle $\phi$ for Monolayer Films**

| compound | $\phi$/deg | $\chi^{(2)} \times 10^7$/ esu | $\beta \times 10^{29}$/ esu | refs |
|---|---|---|---|---|
| *fac*-ClRe(CO)$_3$**L3**[a] | 25.2 | 1.8 | 5.4 | this work |
| BI | 25.0 | 3.9 | 13 | this work |
| BI | 50.0 | 5.1 | 15 | 27 |

[a] Molecular area of 0.48 nm$^2$ and film thickness of 0.23 nm calculated based on molecular modeling. BI = *E*-*N*-methyl-4-(2-(4-octadecyloxyphenyl)ethenyl)pyridinium iodide.

obtained using eqs 2 and 3,[25,27] in which $\theta = 45°$ is the angle of the laser beam to the film; $\chi^{(2)}$ is the second-order susceptibility; $\chi^{(2)}(zzz)$ and $\chi^{(2)}(zxx)$ are the two independent components characterized by the substrate normal (*z*-axis) and *xy* plane on the film surface with the *y*-axis perpendicular to the plane of incidence; $f_{\omega,2\omega}$ = $[(n_{\omega,2\omega})^2 + 2]/3$ is a local field correction factor, where $n_\omega$ and $n_{2\omega}$ are the refractive indices of the film at the fundamental and the second-harmonic frequencies, respectively, with $n_{2\omega}$ usually slightly higher than $n_\omega$. In the actual treatment, $n$ is taken to be $n_\omega \cong n_{2\omega}$ = 1.5; $N = (lA)^{-1}$ is the number of molecules per unit volume, where $l$ is the film thickness and $A$ the molecular area of film-forming materials under study.

The SHG results were summarized in Table 3 and compared with those reported for the monolayer film of *E*-*N*-methyl-4-(2-(4-octadecyloxyphenyl)ethenyl)pyridinium iodide (BI). The $\beta$ value obtained for a film of BI in this work agrees quite well with the value reported in the literature.[27] The $\beta$ value of 5.4 $\times$ 10$^{-29}$ esu obtained for *fac*-ClRe(CO)$_3$**L3** is higher than that observed for the NLO material 2-methyl-4-nitroaniline (4.5 $\times$ 10$^{-29}$ esu).[28] On the contrary, the monolayer film of both *fac*-ClRe(CO)$_3$**L1** and *fac*-ClRe(CO)$_3$**L2** gave very weak SH signals. The SHG parameters for the two

(27) Lupo, D.; Prass, W.; Scheunemann, U.; Laschewsky, A.; Ringsdorf, H.; Ledoux, I. *J Opt. Soc. Am.* B. **1988**, *5*, 300.
(28) Teng, C. C.; Garito, A. F. *Phys. Rev.* B. **1983**, *28*, 6766.

complexes could not be measured with certainty due to their very weak $I_{2\omega}(s \rightarrow p)$ signal. Assuming that the SHG behavior originates from the metal-to-ligand charge transfer (MLCT), one would expect that for *fac*-ClRe-(CO)$_3$**L3** the charge-transfer axis should be tilted away from the film surface normal the most among the complexes *fac*-ClRe(CO)$_3$**L1**, *fac*-ClRe(CO)$_3$**L2**, and *fac*-ClRe(CO)$_3$**L3**, leading to *fac*-ClRe(CO)$_3$**L3** having the worst SHG property. However, the observation of a reverse trend in which a strong SHG signal is found for *fac*-ClRe(CO)$_3$**L3** while weak SHG properties are observed for *fac*-ClRe(CO)$_3$**L1** and *fac*-ClRe(CO)$_3$**L2** is most probably associated with the poor film-forming behavior of these latter two complexes, which does not result in an ordered acentrosymmetric structure.

## Conclusion

Several newly synthesized surfactant Re(I) complexes have been shown to exhibit stable air–water interface behaviors, one of which is capable of forming a stable multilayer LB film on quartz substrate with the monolayer film showing relatively strong second-harmonic signals, which could be ascribed to the good film-forming properties and the metal-to-ligand charge transfer characteristic of the complex.

**Supporting Information Available:** Tables of atomic coordinates, thermal parameters, and all bond distances and angles for complex *fac*-ClRe(CO)$_3$**L4** (9 pages). Ordering information is given on any current masthead page.

OM970998F